Structure and Transitions of Light Nuclei

Robert B. Wiringa, Physics Division, Argonne National Laboratory

Joseph Carlson, Los Alamos
Stefano Gandolfi, Los Alamos
Diego Lonardoni, Michigan State
Alessandro Lovato, Argonne
Saori Pastore, Los Alamos
Maria Piarulli, Argonne
Steven C. Pieper, Argonne
Rocco Schiavilla, JLab & ODU

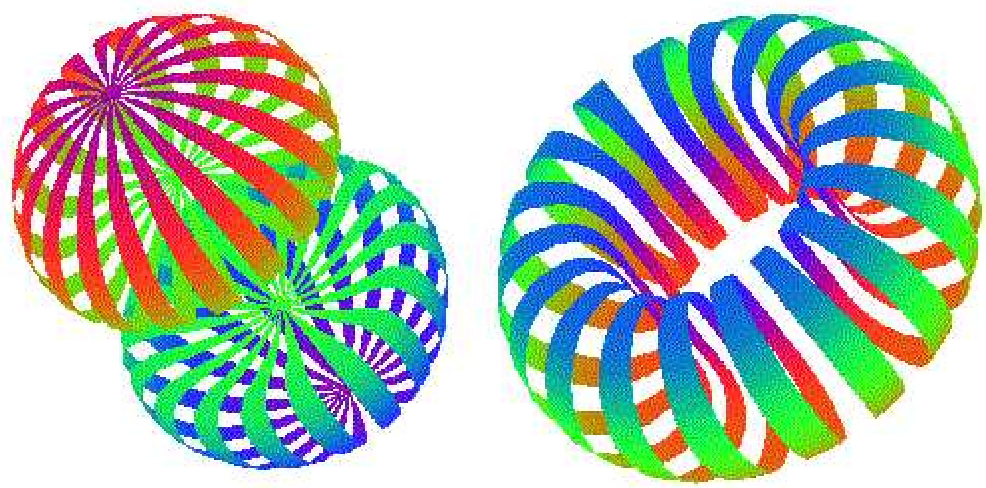

WORK NOT POSSIBLE WITHOUT EXTENSIVE COMPUTER RESOURCES

Argonne Laboratory Computing Resource Center (Blues)
Argonne Leadership Computing Facility (Mira & Theta)

Argonne NATIONAL LABORATORY

Physics Division

Work supported by U.S. Department of Energy, Office of Nuclear Physics

Ab Initio Calculations of Light Nuclei

Goals

Understand nuclei at the level of elementary interactions between individual nucleons, including

- Binding energies, excitation spectra, relative stability
- Densities, electromagnetic moments, transition amplitudes, cluster-cluster overlaps
- Low-energy NA & AA' scattering, asymptotic normalizations, astrophysical reactions

Requirements

- Two-nucleon potentials that accurately describe elastic NN scattering data
- Consistent three-nucleon potentials and electroweak current operators
- Accurate methods for solving the many-nucleon Schrödinger equation

Results

- Quantum Monte Carlo methods can evaluate realistic Hamiltonians accurate to $\sim$1–2%
- About 100 states calculated for $A \leq 12$ nuclei in good agreement with experiment
- Applications to elastic & ineleastic e, π scattering, $(e, e'p)$, (d, p) reactions, etc.
- Electromagnetic moments, $M1$, $E2$, F, GT transitions, electroweak response
- ^{5}He = $n\alpha$ scattering and $3 \leq A \leq 9$ ANCs and widths

NUCLEAR HAMILTONIAN

$$H = \sum_i K_i + \sum_{i<j} v_{ij} + \sum_{i<j<k} V_{ijk}$$

K_i: Non-relativistic kinetic energy, m_n-m_p effects included

Argonne v$_{18}$: $v_{ij} = v_{ij}^{\gamma} + v_{ij}^{\pi} + v_{ij}^{I} + v_{ij}^{S} = \sum v_p(r_{ij}) O_{ij}^p$

- 18 spin, tensor, spin-orbit, isospin, etc., operators
- full EM and strong CD and CSB terms included
- predominantly local operator structure
- fits Nijmegen PWA93 data with χ^2/d.o.f.=1.1

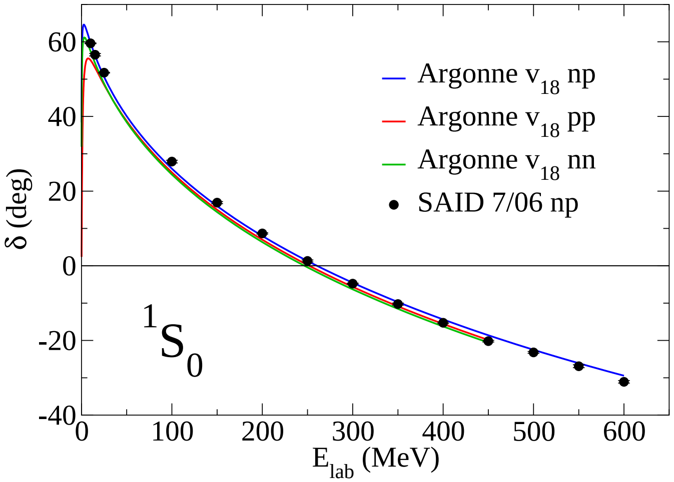

Wiringa, Stoks, & Schiavilla, PRC **51**, (1995)

Urbana & Illinois: $V_{ijk} = V_{ijk}^{2\pi} + V_{ijk}^{3\pi} + V_{ijk}^{R}$

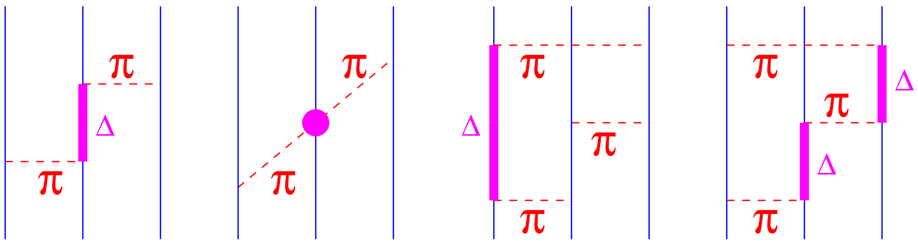

- Urbana has standard 2π P-wave + short-range repulsion for matter saturation
- Illinois adds 2π S-wave + 3π rings to provide extra T=3/2 interaction
- Illinois-7 has four parameters fit to 23 levels in $A \leq 10$ nuclei

Pieper, Pandharipande, Wiringa, & Carlson, PRC **64**, 014001 (2001)

Pieper, AIP CP **1011**, 143 (2008)

QUANTUM MONTE CARLO

Variational Monte Carlo (VMC): construct Ψ_V that

- Are fully antisymmetric and translationally invariant
- Have cluster structure and correct asymptotic form
- Contain non-commuting 2- & 3-body operator correlations from v_{ij} & V_{ijk}
- Are orthogonal for multiple J^π states
- Minimize $E_V = \langle \Psi_V | H | \Psi_V \rangle \geq E$

These are $\sim 2^A \binom{A}{Z}$ component (540,672 for ^{12}C) spin-isospin vectors in $3A$ dimensions

Green's function Monte Carlo (GFMC): project out the exact eigenfunction

- $\Psi(\tau) = \exp[-(H - E_0)\tau]\Psi_V = \sum_n \exp[-(E_n - E_0)\tau] a_n \Psi_n \Rightarrow \Psi_0$ at large τ
- Propagation done stochastically in small time slices $\Delta\tau$
- Exact $\langle H \rangle$ for local potentials; mixed estimates for other $\langle O \rangle$
- Constrained-path propagation controls fermion sign problem for $A \geq 8$
- Multiple excited states for same J^π stay orthogonal

Many tests demonstrate 1–2% accuracy for realistic $\langle H \rangle$

Carlson, *et al.*, RMP **87**, 1067 (2015)

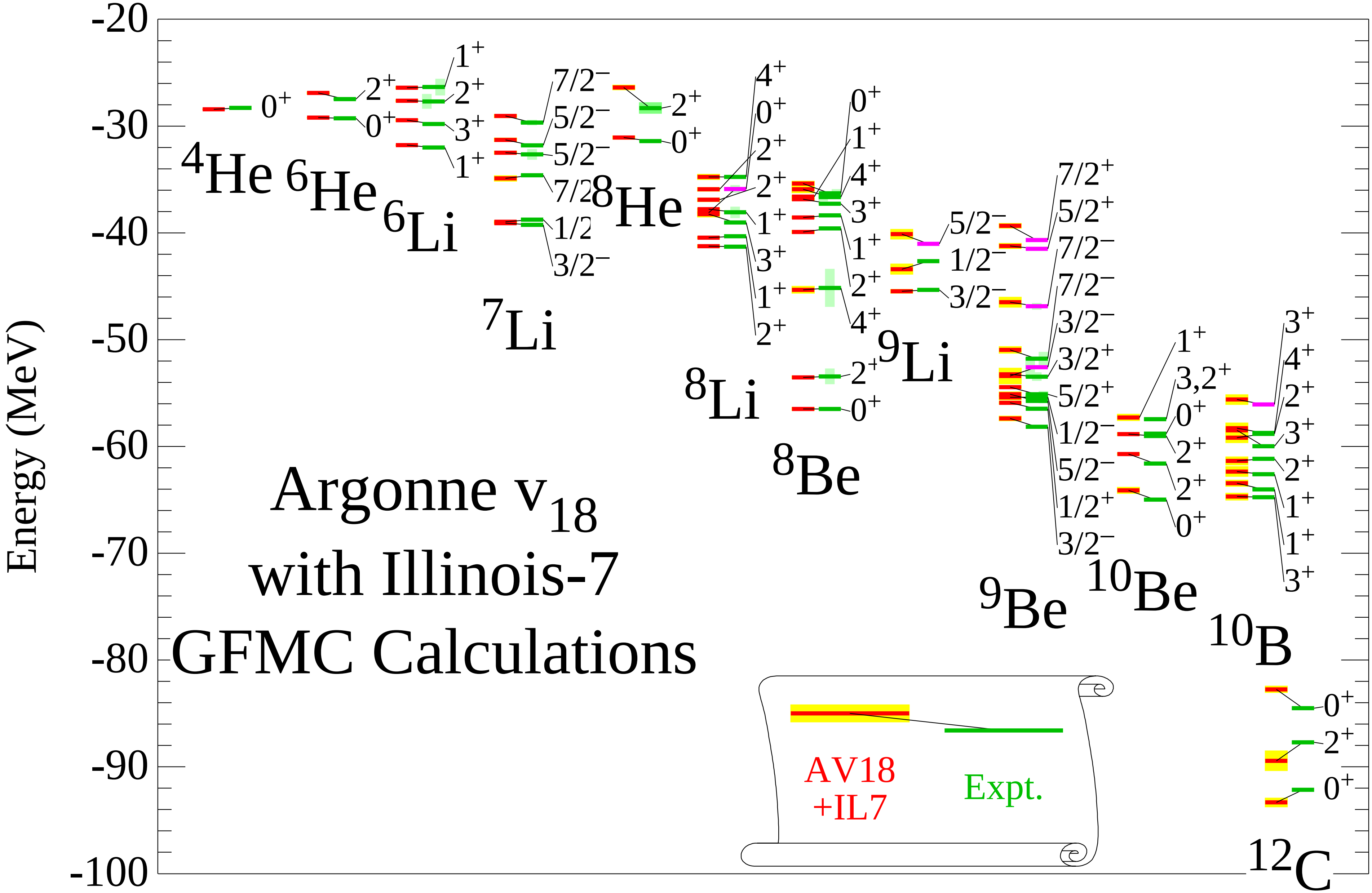
Energy (MeV)
-20
-30
-40
-50
-60
-70
-80
-90
-100
4He
6He
6Li
7Li
8He
8Li
8Be
9Li
9Be
10Be
10B
12C
Argonne v18
with Illinois-7
GFMC Calculations
AV18
+IL7
Expt.

NOLEN-SCHIFFER ANOMALY

Nuclear forces are mostly charge-independent [CI $\propto 1, \tau_i \cdot \tau_j$], but have small charge-dependent [CD $\propto T_{ij}$] and charge-symmetry-breaking [CSB $\propto (\tau_i + \tau_j)_z$] components, while electromagnetic forces are a mix of CI, CD, & CSB terms. Evidence for strong charge-independence-breaking (CIB) comes from the energy differences of isobaric multiplets:

$$E_{A,T}(T_z) = \sum_{n \leq 2T} a_n(A,T) Q_n(T,T_z)$$

$$Q_0 = 1 \; ; \; Q_1 = T_z \; ; \; Q_2 = \tfrac{1}{2}(3T_z^2 - T^2)$$

For example,

$$a_1(3, \tfrac{1}{2}) = E(^3\text{He}) - E(^3\text{H}) \qquad a_2(6,1) = \tfrac{1}{3}[E(^6\text{Be}) - 2E(^6\text{Li}^*) + E(^6\text{He})]$$

The Nolen-Schiffer anomaly is the difference not explained by Coulomb force; strong CIB and other electromagnetic terms in Argonne v_{18} explain much of the remainder (shown in keV):

$a_n(A,T)$	K^{CSB}	$v_{C1}(pp)$	$v^{\gamma,R}$	v^{CSB} $+v^{CD}$	δH^{CI}	Total	Expt.
$a_1(3,\frac{1}{2})$	14	642(1)	26	65(0)	8(1)	755(1)	764
$a_1(7,\frac{1}{2})$	23	1442(2)	36	83(1)	27(10)	1611(10)	1645
$a_1(8,1)$	25	1652(3)	18	77(1)	33(11)	1813(11)	1770
$a_2(6,1)$		140(1)	18	100(2)	17(2)	273(3)	223
$a_2(8,1)$		133(1)	3	−3(2)	10(5)	139(5)	127

Isospin-mixing in ^{8}Be

Experimental energies of 2^+ states

E_a = 16.626(3) MeV Γ_a^α = 108.1(5) keV

E_b = 16.922(3) MeV Γ_b^α = 74.0(4) keV

Isospin mixing of 2^+;1 and 2^+;0* states due to isovector interaction H_{01}:

$\Psi_a = \beta\Psi_0 + \gamma\Psi_1$; $\Psi_b = \gamma\Psi_0 - \beta\Psi_1$

decay through $T = 0$ component only

$\Gamma_a^\alpha / \Gamma_b^\alpha = \beta^2/\gamma^2 \Rightarrow \beta = 0.77$; $\gamma = 0.64$

$$E_{a,b} = \frac{H_{00} + H_{11}}{2} \pm \sqrt{\left(\frac{H_{00} - H_{11}}{2}\right)^2 + (H_{01})^2}$$

$H_{00} = 16.746(2)$ MeV

$H_{11} = 16.802(2)$ MeV

$H_{01} = -145(3)$ keV

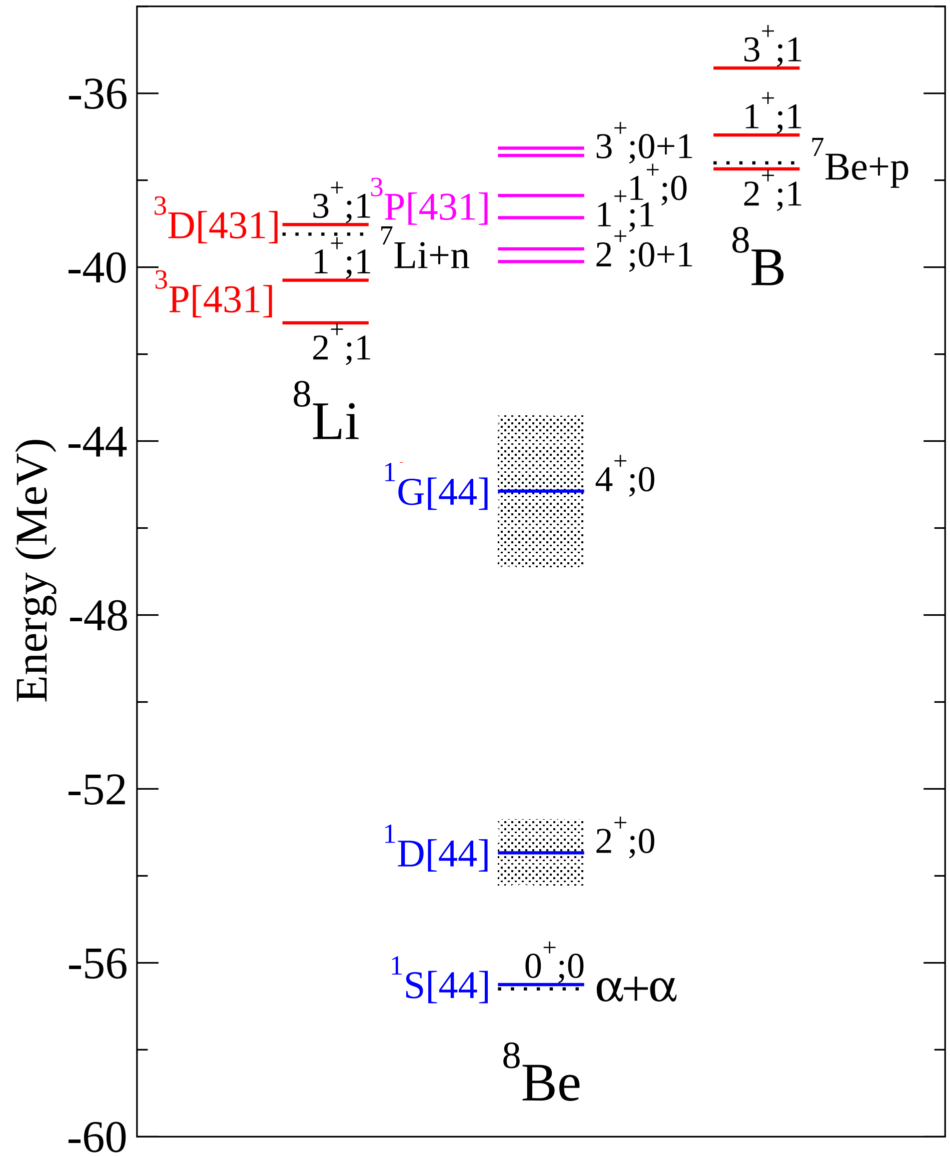

Isospin-mixing matrix elements in keV

	K^{CSB}	$v_{C1}(pp)$	$v^{\gamma,R}$	$v^{CSB}+v^{CD}$	H_{01}	Expt.
$2^+;1\Leftrightarrow 2_2^+;0$	$-3.6(1)$	$-89.3(11)$	$-11.0(2)$	$-23.4(4)$	$-127(2)$	$-145(3)$
$1^+;1\Leftrightarrow 1^+;0$	$-2.8(1)$	$-73.4(11)$	$1.0(1)$	$-18.5(4)$	$-94(1)$	$-103(14)$
$3^+;1\Leftrightarrow 3^+;0$	$-3.0(1)$	$-74.6(12)$	$-16.8(2)$	$-16.6(4)$	$-111(2)$	$-59(12)$
$2^+;1\Leftrightarrow 2_1^+;0$					$-7(2)$	
$0^+;2\Leftrightarrow 0_3^+;0$		$-32.2(2)$	$-8.9(1)$	$-83.8(22)$	$-125(2)$	

Coulomb terms are 70% of H_{01}, but magnetic moment and strong Type III CSB are relatively more important than in Nolen-Schiffer anomaly; still missing $\approx 10\%$ of strength.

Strong Type IV CSB also contribute (probably best nuclear structure place to look):

$$V_{IV}^{CSB} = (\tau_1 - \tau_2)_z(\sigma_1 - \sigma_2)\cdot \mathbf{L}\, v(r) + (\tau_1 \times \tau_2)_z(\sigma_1 \times \sigma_2)\cdot \mathbf{L}\, w(r)$$

These contributions are model-dependent with $V_{IV}^{CSB} \sim \pm$ few keV.

Wiringa, Pastore, Pieper, & Miller, Phys. Rev. C **88**, 044333 (2013)

$A \leq 10$ Magnetic moments w/ χEFT exchange currents

Hybrid calculations using AV18+IL7 wave functions and χEFT exchange currents developed in:

Pastore, Schiavilla, & Goity, PRC **78**, 064002 (2008) ; Pastore, *et al.*, PRC **80**, 034004 (2009)

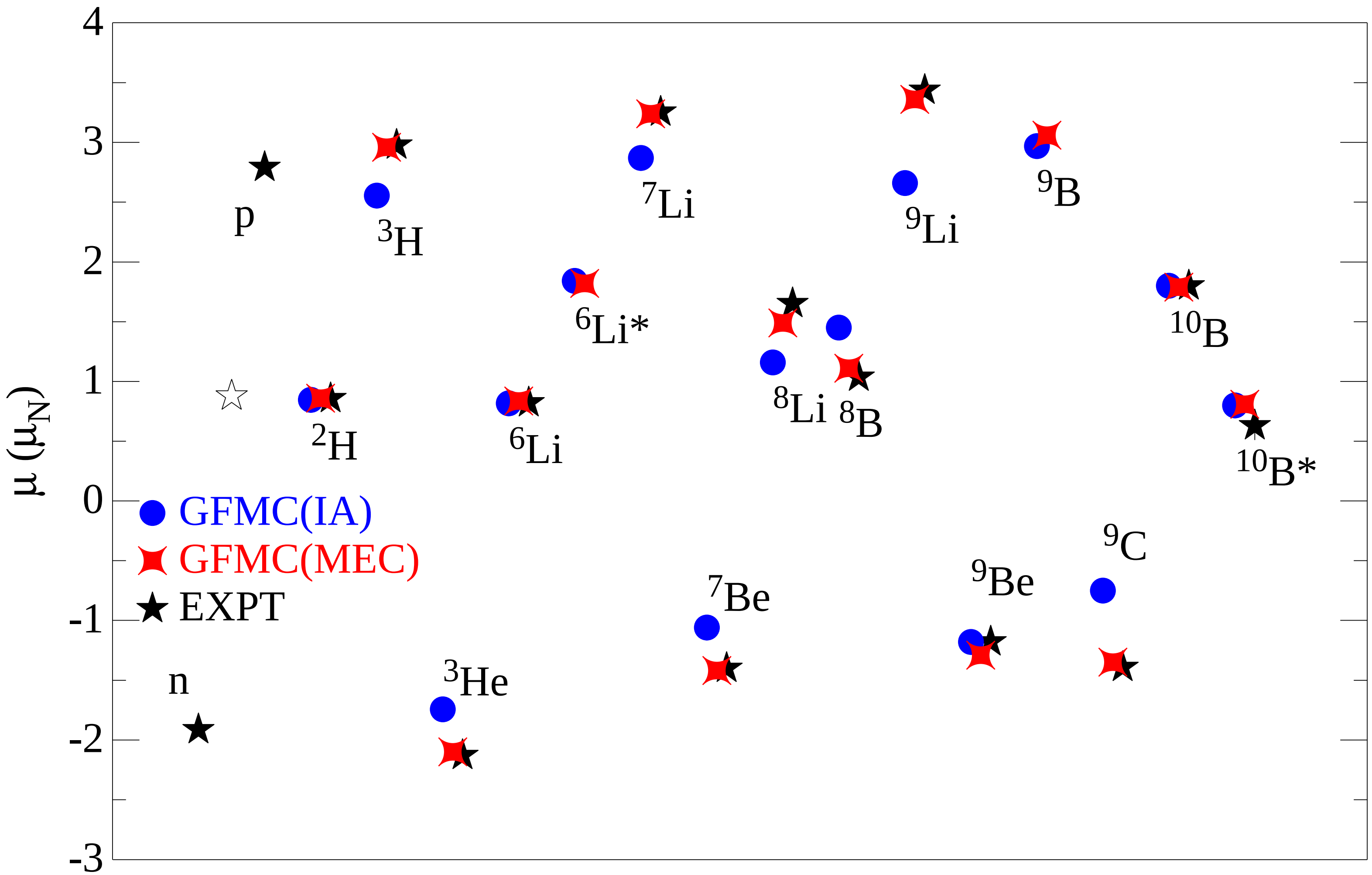

Pastore, Pieper, Schiavilla & Wiringa, PRC **87**, 035503 (2013)

Single-nucleon densities

$$\rho_{p,n}(r) = \sum_i \langle\Psi|\delta(r - r_i)\frac{1 \pm \tau_i}{2}|\Psi\rangle$$

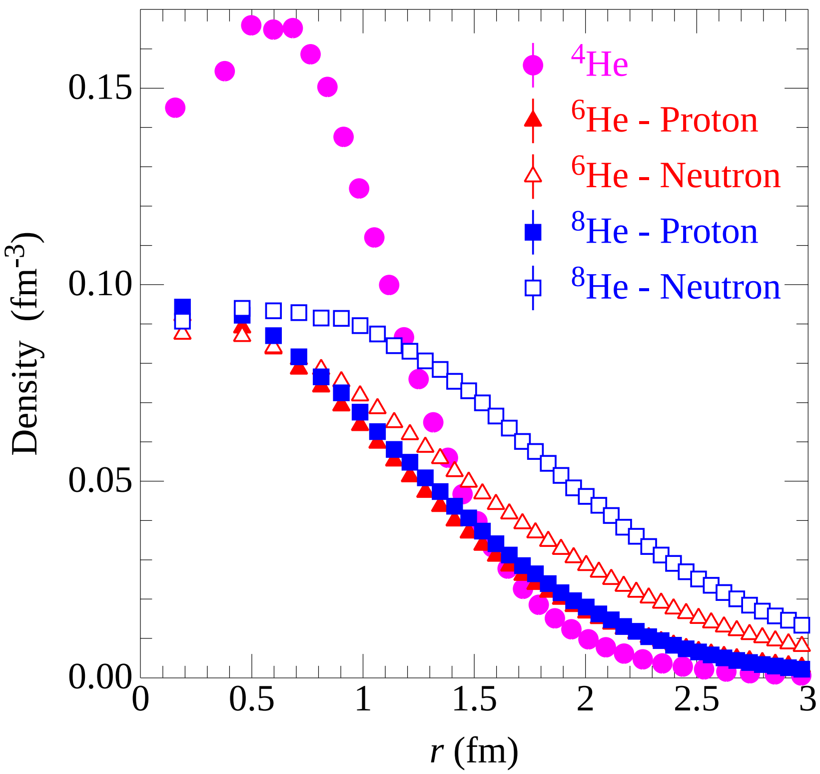

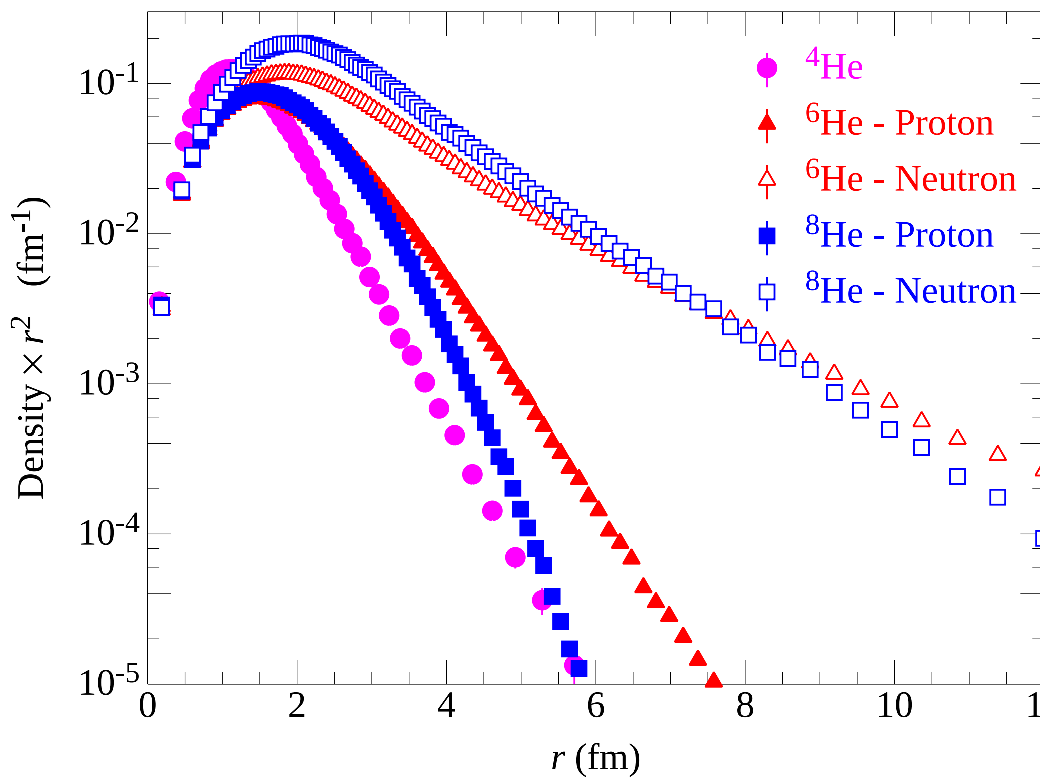

RMS radii

	r_n	r_p	r_c	Expt
^{4}He	1.45(1)	1.45(1)	1.67(1)	1.681(4)*
^{6}He	2.86(6)	1.92(4)	2.06(4)	2.060(8)†
^{8}He	2.79(3)	1.82(2)	1.94(2)	1.959(16)‡

*Sick, PRC **77**, 041302(R) (2008)

†Wang, *et al.*, PRL **93**, 142501 (2004)

‡Mueller, *et al.*, PRL **99**, 252501 (2007)

Brodeur, *et al.*, PRL **108**, 052504 (2012)

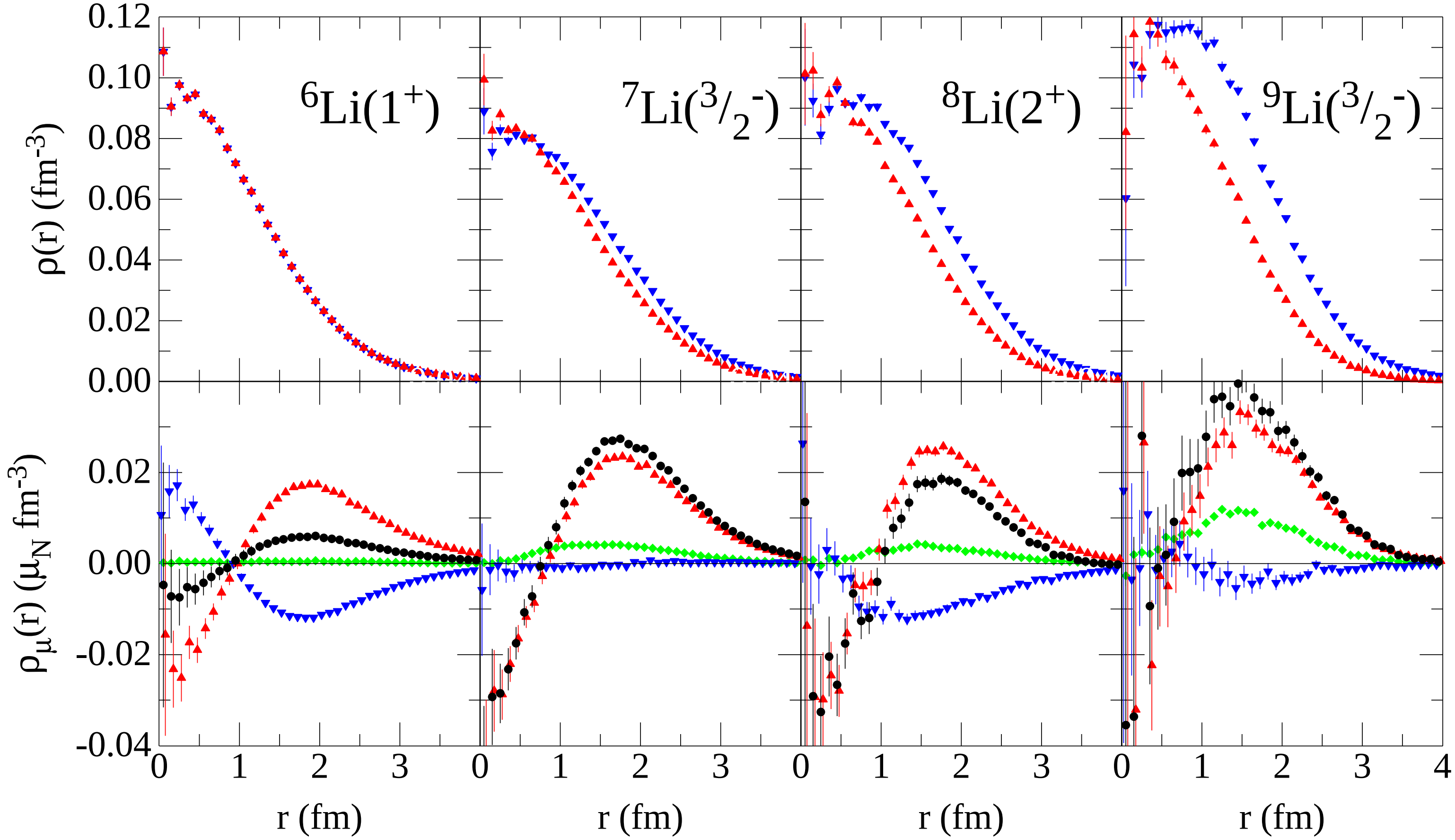

RMS radii

	r_c	Expt	r_m	Expt
^{6}Li	2.53(1)	2.589(39)*	3.30(2)	
^{7}Li	2.38(1)	2.444(43)*	2.86(2)	2.98(5) †
^{8}Li	2.24(1)	2.339(45)*	1.85(2)	
^{9}Li	2.10(1)	2.245(47)*	2.38(2)	

* Nörtershauser, *et al.*, PRC **84**, 024307(R) (2011)

†Van Niftrik, *et al.*, NPA **174**, 173 (1971)

Two-nucleon densities

$$\rho_{pp}(r) = \sum_{i<j} \langle \Psi | \delta(r - |\mathbf{r}_i - \mathbf{r}_j|) \frac{1+\tau_i}{2} \frac{1+\tau_j}{2} | \Psi \rangle$$

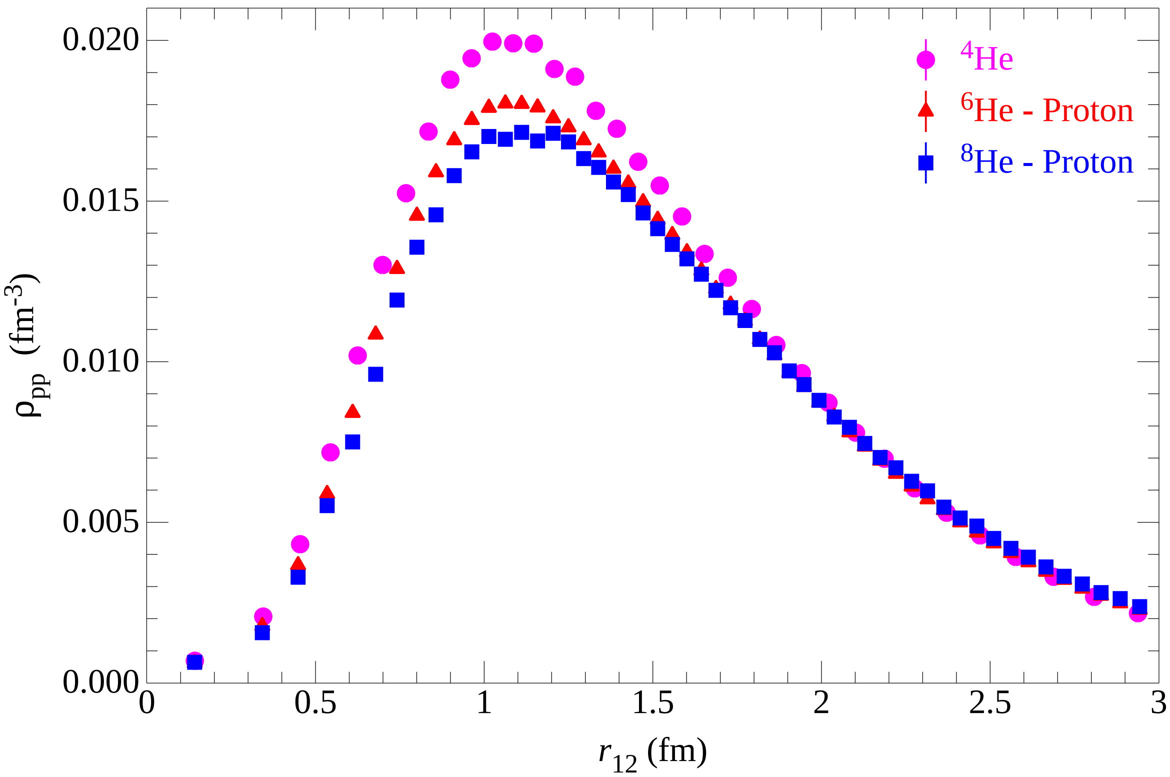

RMS radii

	r_{pp}	r_{np}	r_{nn}
^{4}He	2.41	2.35	2.41
^{6}He	2.51	3.69	4.40
^{8}He	2.52	3.58	4.37

INTRINSIC DENSITY OF ^{8}BE

^{8}Be w.f.: ^{4}He core + 4 p-shell nucleons + pair corr.

M. C. $\rho(\mathbf{r})$: random walk in $|\Psi(\mathbf{r}_1, \mathbf{r}_2, \cdots, \mathbf{r}_8)|^2$ & periodically for each set $(\mathbf{r}_1, \mathbf{r}_2, \cdots, \mathbf{r}_8)$

Lab $\rho(\mathbf{r})$: bin $\mathbf{r}_1, \mathbf{r}_2, \cdots, \mathbf{r}_8$

Intrinsic $\rho(\mathbf{r})$: find eigenvectors of moment of inertia matrix:

$$\mathcal{M} = \sum_i \begin{pmatrix} x_i^2 & x_i y_i & x_i z_i \\ y_i x_i & y_i^2 & y_i z_i \\ z_i x_i & z_i y_i & z_i^2 \end{pmatrix} ,$$

rotate to them, and bin $\mathbf{r}'_1, \mathbf{r}'_2, \cdots, \mathbf{r}'_8$.

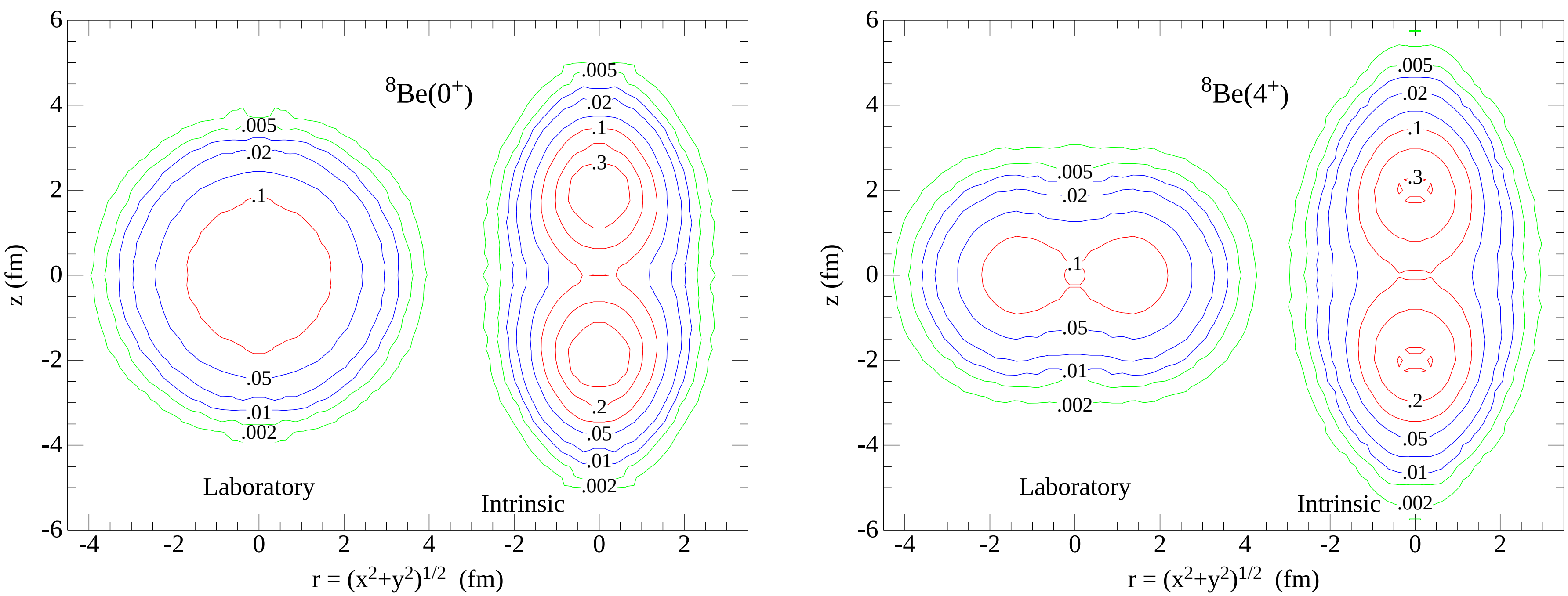

Wiringa, Pieper, Carlson, & Pandharipande, Phys. Rev. C **62**, 014001 (2000)

Two-nucleon halo densities

$$\rho_{nn}(r) = \sum_{i<j} \langle \Psi(J^\pi, T, T_z = +1) | \delta(r - |\mathbf{r}_i - \mathbf{r}_j|) \tau_i^+ \tau_j^+ | \Psi(J^\pi, T, T_z = -1) \rangle$$

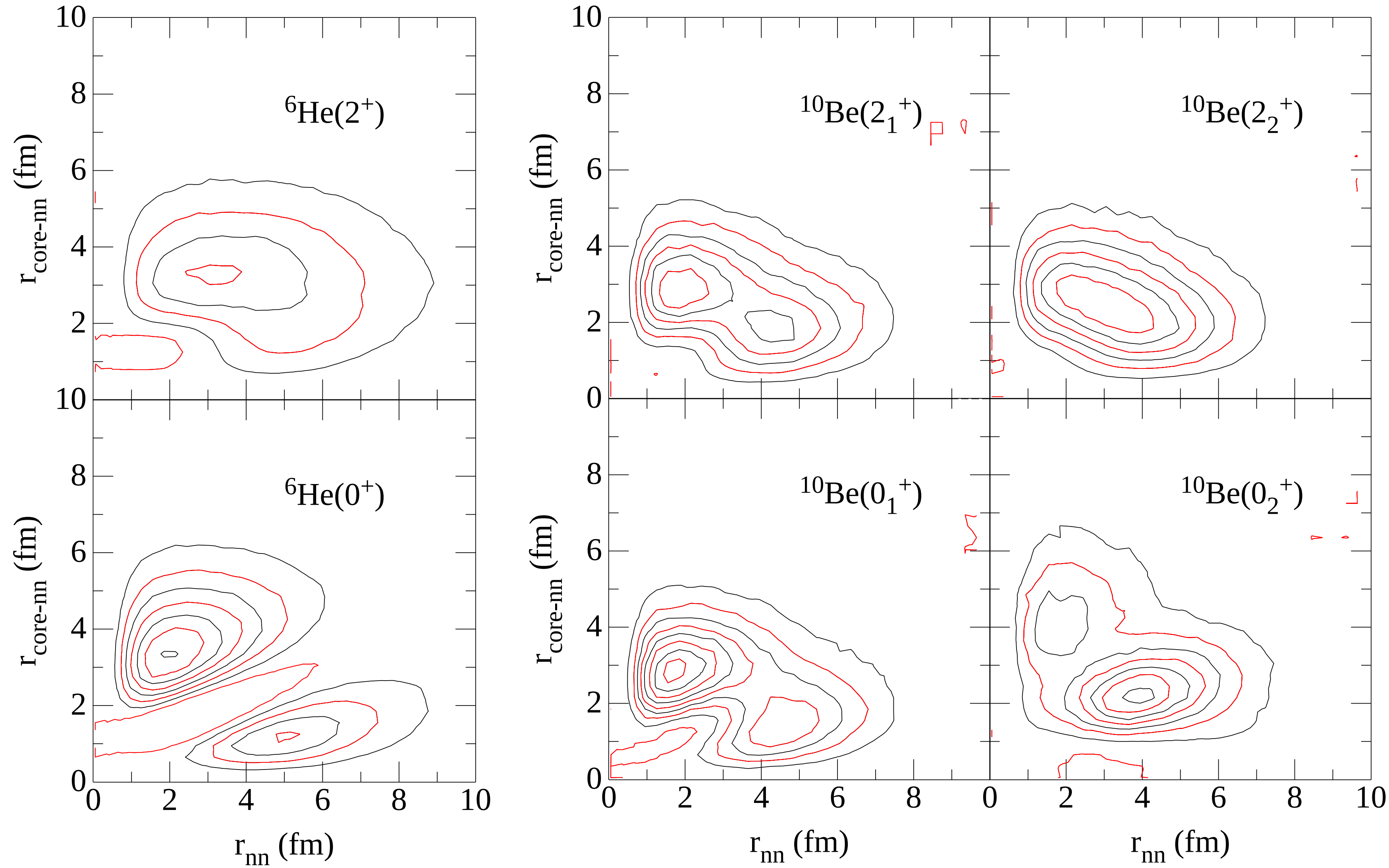

SINGLE-NUCLEON MOMENTUM DISTRIBUTIONS

Probability of finding a nucleon in a nucleus with momentum k in a given spin-isospin state:

$$\rho_{\sigma\tau}(k) = \int d\mathbf{r}'_1 d\mathbf{r}_1 d\mathbf{r}_2 \cdots d\mathbf{r}_A \, \psi^\dagger_A(\mathbf{r}'_1, \mathbf{r}_2, \ldots, \mathbf{r}_A) \, e^{-i\mathbf{k}\cdot(\mathbf{r}_1 - \mathbf{r}'_1)} \, P_{\sigma\tau} \, \psi_A(\mathbf{r}_1, \mathbf{r}_2, \ldots, \mathbf{r}_A)$$

- Useful input for electron scattering studies
- Universal character of high-momentum tails from np tensor interaction

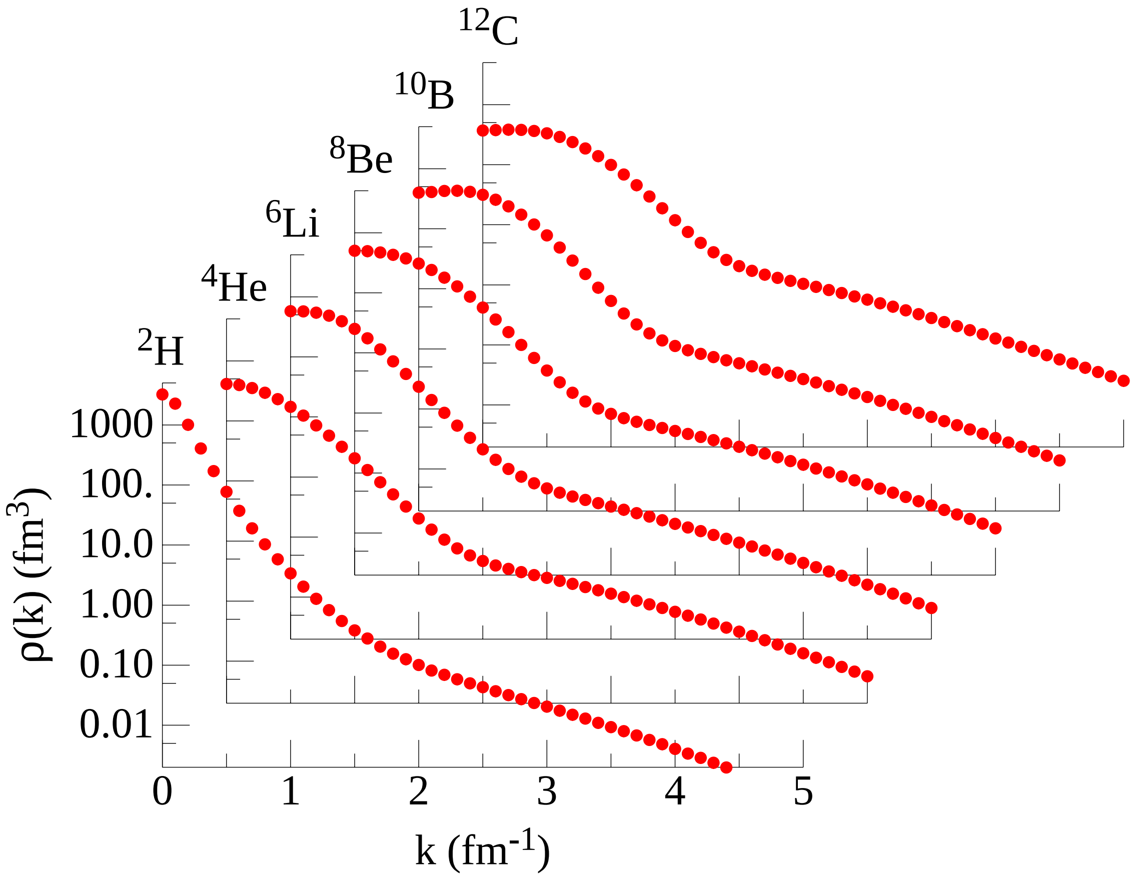

Wiringa, Schiavilla, Pieper, & Carlson, PRC **89**, 024305 (2014)

Two-nucleon momentum distributions

Probability $\rho_{NN}(q, Q)$ of finding a pair of nucleons with relative momentum q and total momentum Q can be defined in a similar fashion:

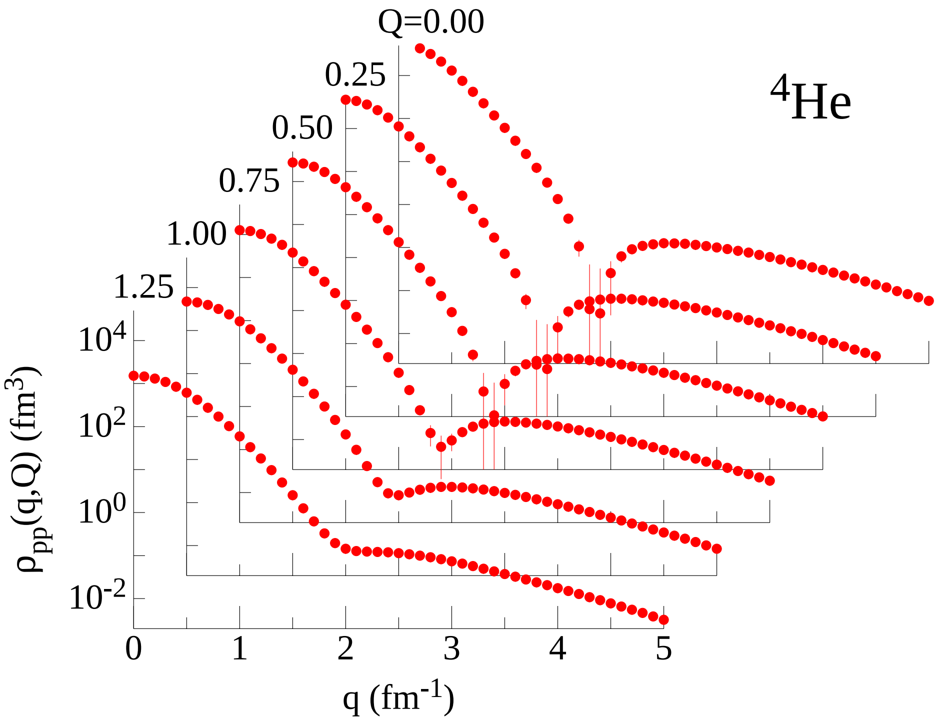

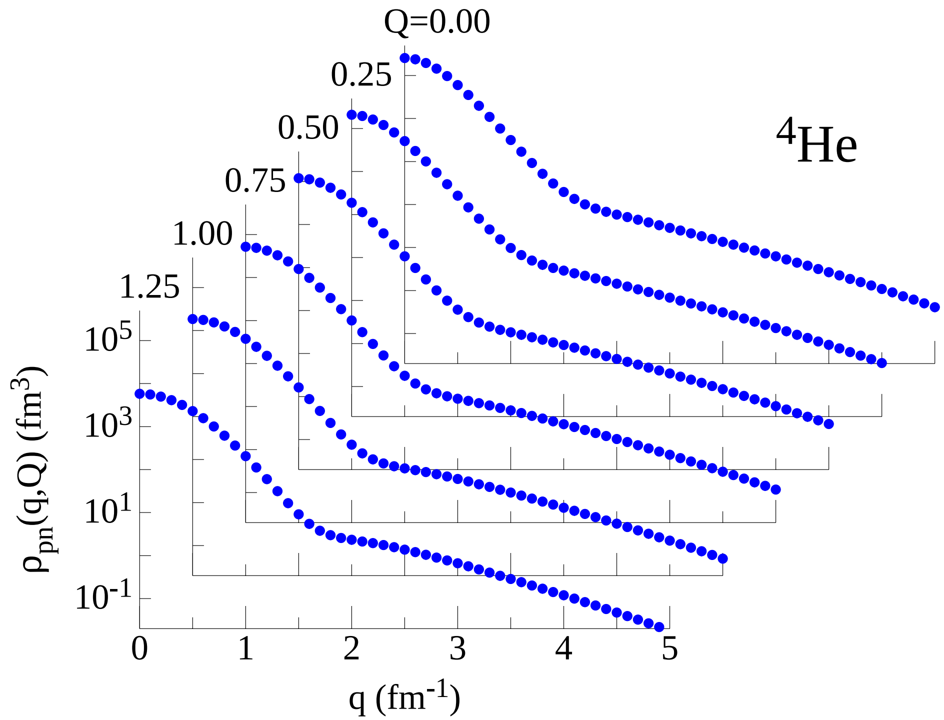

- Large ratio $\rho_{pn}(q, Q = 0)$ / $\rho_{pp}(q, Q = 0)$ has been observed in ^{12}C$(e, e'pN)$ scattering
- Results in good agreement with recent ^{4}He$(e, e'pN)$ experiment

Korover, *et al.* (JLab Hall A), PRL **113**, 022501 (2014)

$M1$, $E2$, F, GT transitions

NO EFFECTIVE CHARGES!

$$E2 = e\sum_k \tfrac{1}{2}\left[r_k^2 Y_2(\hat{r}_k)\right](1+\tau_{kz})$$

$$M1 = \mu_N \sum_k [(L_k + g_p S_k)(1+\tau_{kz})/2 + g_n S_k \ (1-\tau_{kz})/2]$$

$$\mathrm{F} = \sum_k \tau_{k\pm} \ ; \ \mathrm{GT} = \sum_k \sigma_k \tau_{k\pm}$$

Pervin, Pieper, & Wiringa, PRC **76**, 064319 (2007)

Marcucci, Pervin, *et al.*, PRC **78**, 065501 (2008)

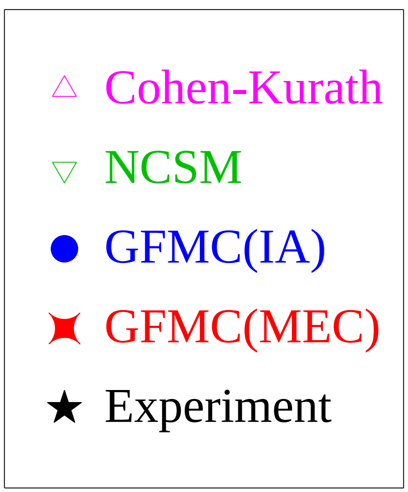

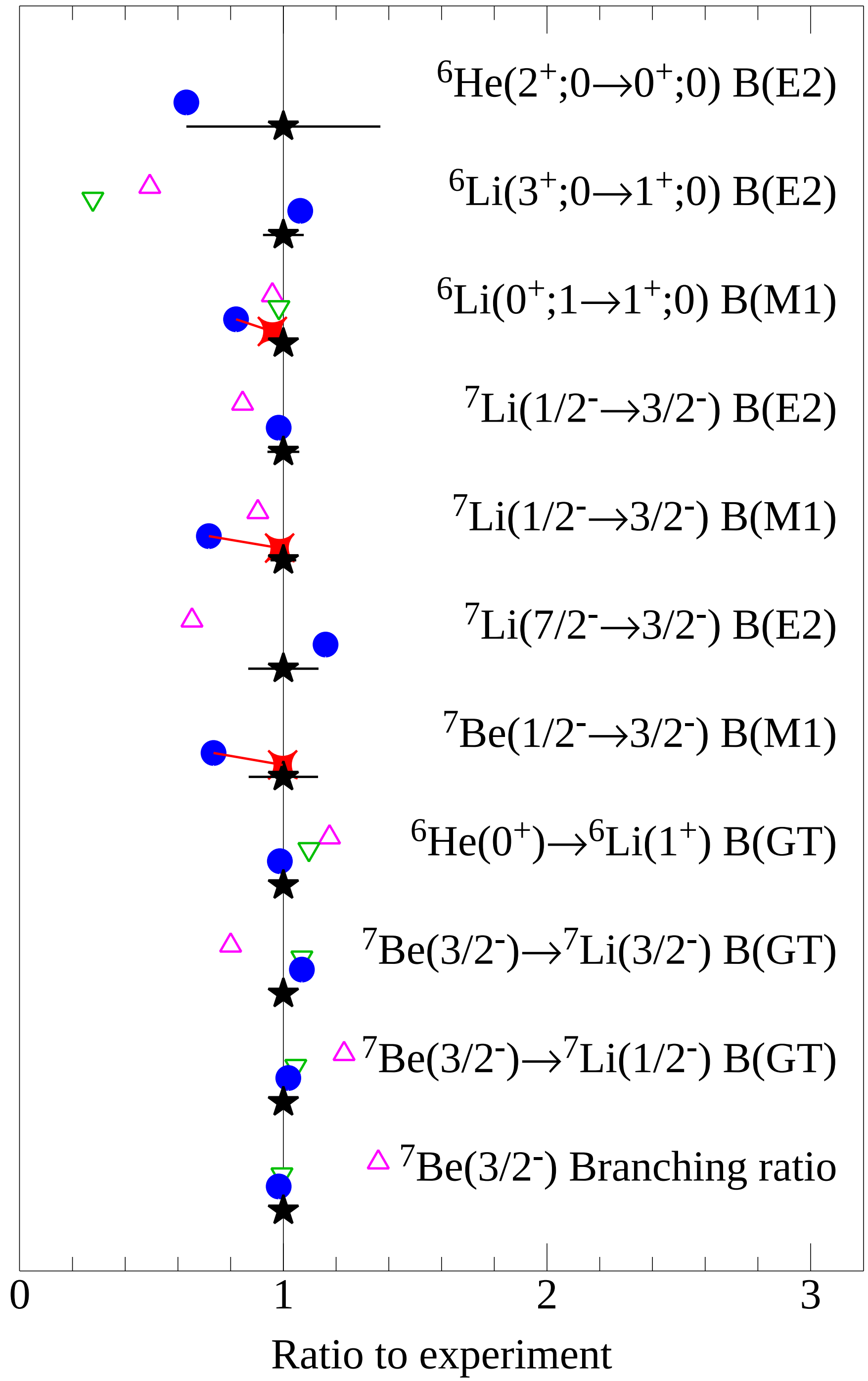

$M1$ TRANSITIONS W/ χEFT

- dominant contribution is from OPE
- five LECs at N3LO
- d_2^V and d_1^V are fixed assuming Δ resonance saturation
- d^S and c^S are fit to experimental μ_d and $\mu_S(^3\text{H}/^3\text{He})$
- c^V is fit to experimental $\mu_V(^3\text{H}/^3\text{He})$
- $\Lambda = 600$ MeV

Pastore, Pieper, Schiavilla, & Wiringa

PRC **87**, 035503 (2013)

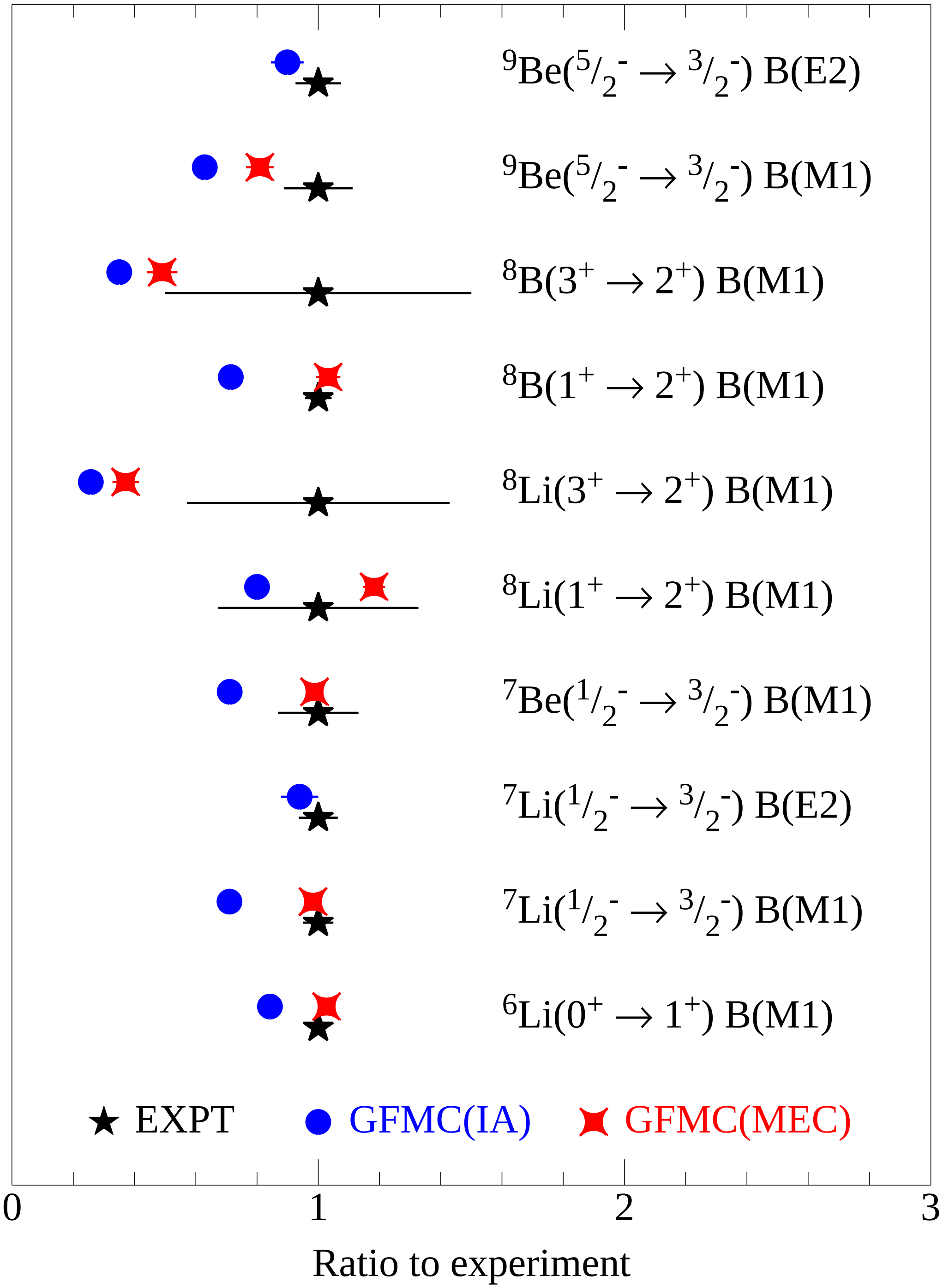

M1 TRANSITION DENSITIES

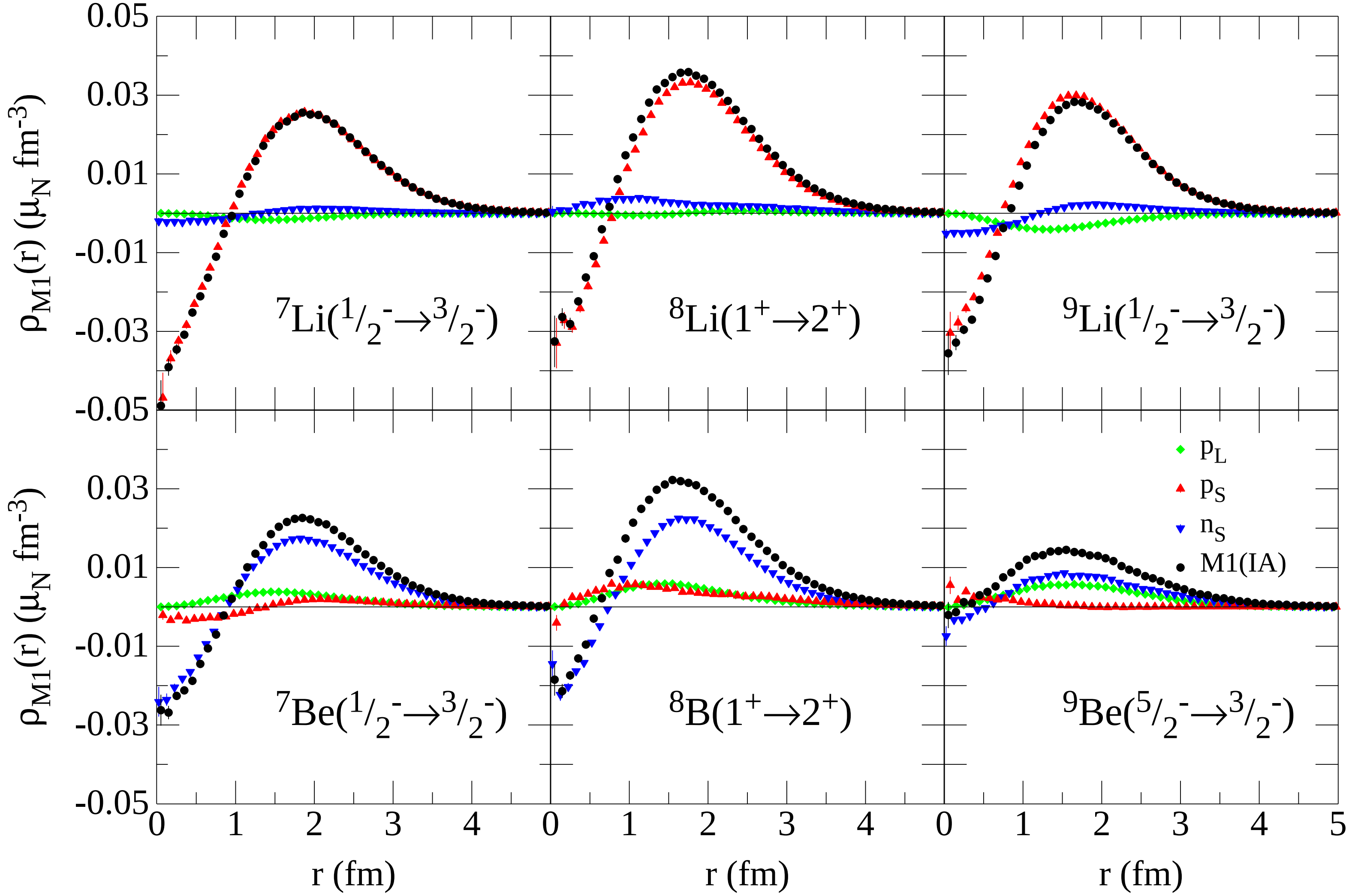

$\mu_p[\rho_{p\uparrow}(r) - \rho_{p\downarrow}(r)]$ $\mu_n[\rho_{n\uparrow}(r) - \rho_{n\downarrow}(r)]$ $\mu_p \rho_{p\mathbf{L}}(r)$

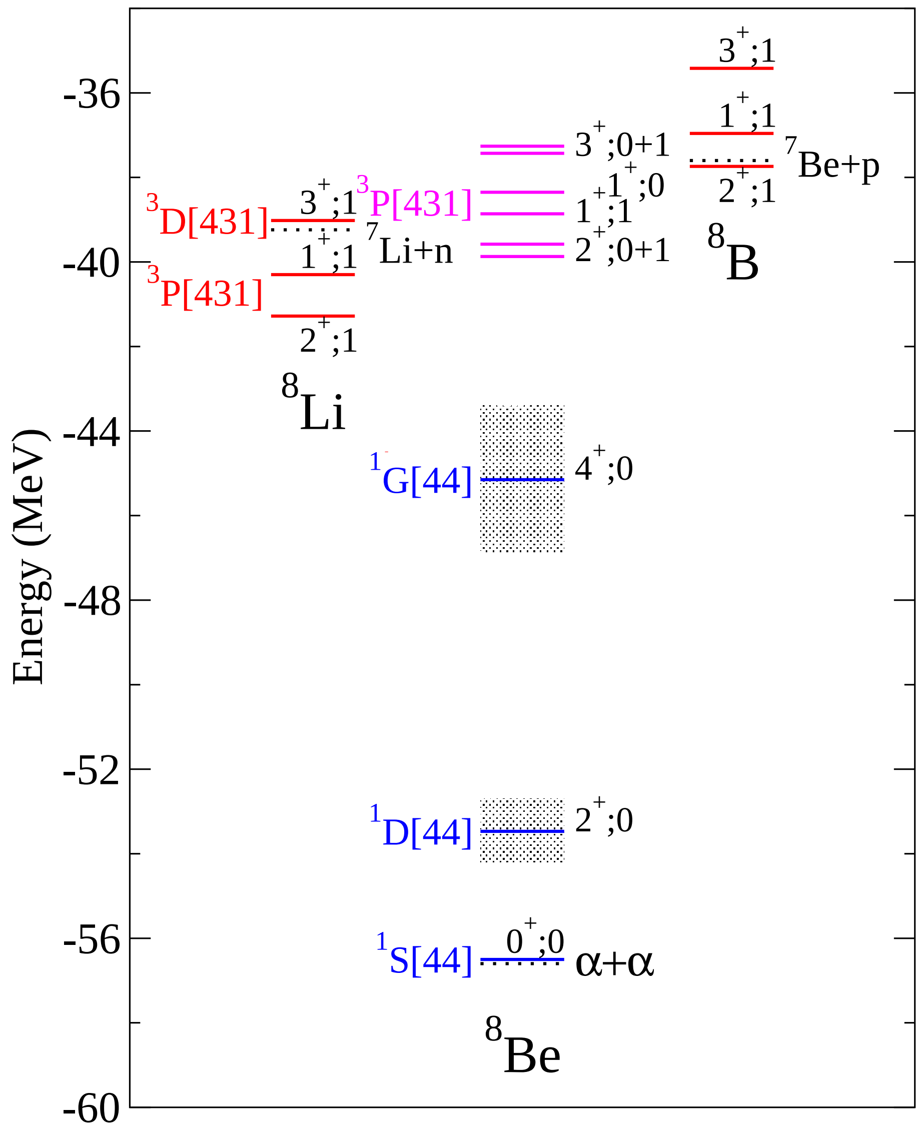

TRANSITIONS IN/TO ^{8}Be

- ^{8}Be presents new challenges in transition calculations
- $E2$ transitions between rotational band states which have large widths
- $M1$ transitions involving isospin-mixed states
- GT transitions that are not super-allowed and go to a broad final state

$J^\pi;T$	GFMC	Expt
0^+	-56.3(2)	-56.50
2^+	+ 3.2(2)	+ 3.03(1)
4^+	+11.2(2)	+11.35(15)
$2^+;0$	+16.8(3)	+16.746(3) $\longrightarrow$ 16.626
$2^+;1$	+16.8(3)	+16.802(3) $\longrightarrow$ 16.922
$1^+;1$	+17.4(2)	+17.66(1) $\longrightarrow$ 17.64
$1^+;0$	+18.0(3)	+18.13(1) $\longrightarrow$ 18.15

$E2$ TRANSITIONS IN ^{8}Be

- New experiment at Tata Institute, Mumbai for $4^+ \to 2^+$ transition
- Experimental AND theoretical challenge: 4^+ and 2^+ states are wide and breakup into two αs
- GFMC calculation is extrapolated back to $\tau = 0.1$ MeV^{-1}; predicts $B(E2)$ = 27.2(15)
- Experiment detects α+α+γ in coincidence for range of beam energies
- Assuming Breit-Wigner shape, simple analysis gives $B(E2)$ = 21.3(23)

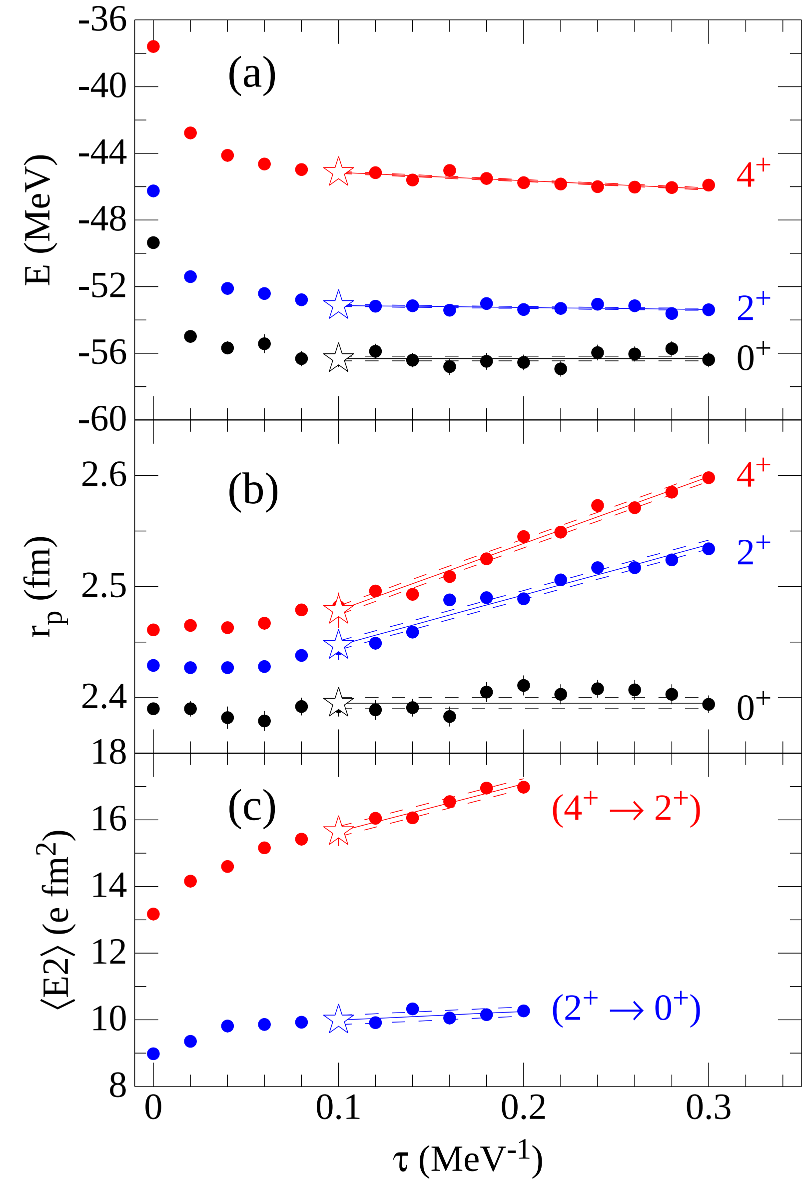

Datar, Chakrabarty, Kumar, Nanal, Pastore, Wiringa, et al., PRL **111**, 062502 (2013)

$M1$ TRANSITIONS IN ^{8}Be BETWEEN ISOSPIN-MIXED STATES

We calculate between states of pure isospin:

matrix element	IA	MEC	TOT
$\langle 1^+;1\|M1\|2^+;0\rangle$	2.29(1)	0.62(1)	2.91(1)
$\langle 1^+;1\|M1\|2^+;1\rangle$	0.14(0)	0.04(1)	0.18(1)
$\langle 1^+;0\|M1\|2^+;0\rangle$	0.17(0)	0.02(0)	0.19(0)
$\langle 1^+;0\|M1\|2^+;1\rangle$	2.60(1)	0.29(1)	2.89(1)

Then have to combine them using the physical states:

$$|16.626\rangle = 0.77|2^+;0\rangle + 0.64|2^+;1\rangle \qquad |17.64\rangle = 0.24|1^+;0\rangle + 0.97|1^+;1\rangle$$
$$|16.922\rangle = 0.64|2^+;0\rangle - 0.77|2^+;1\rangle \qquad |18.15\rangle = 0.97|1^+;0\rangle - 0.24|1^+;1\rangle$$

to get the final results:

$B(M1)$	IA	TOT	Expt
17.64 $\longrightarrow$ 16.626	1.65(2)	2.54(3)	2.65(25)
17.64 $\longrightarrow$ 16.922	0.25(1)	0.46(1)	0.30(7)
18.15 $\longrightarrow$ 16.626	0.56(1)	0.62(1)	1.88(46)
18.15 $\longrightarrow$ 16.922	1.56(2)	2.01(2)	2.89(33)

We evaluate the isospin-mixing matrix elements $\langle H_{01}\rangle$ to make sure we have the correct relative signs of our wave functions.

M1 TRANSITION DENSITIES

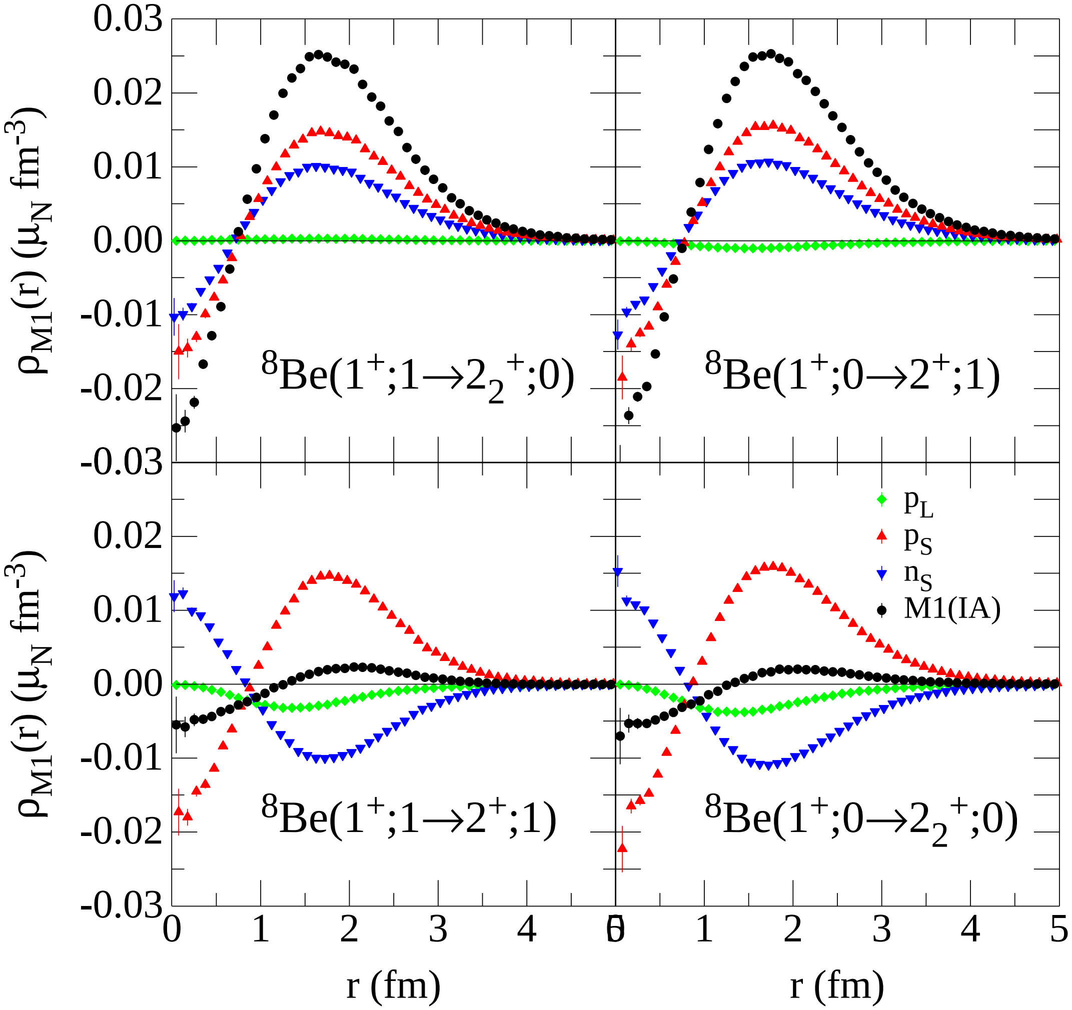

$\mu_p[\rho_{p\uparrow}(r) - \rho_{p\downarrow}(r)]$ $\mu_n[\rho_{n\uparrow}(r) - \rho_{n\downarrow}(r)]$ $\mu_p \rho_{p\mathbf{L}}(r)$

Weak decays

Preliminary results for single β decays:

$^{A}Z(J^{\pi},T)$ Q	F VMC	F GFMC	GT VMC	GT GFMC	Expt Chou	Expt Suzuki
$^{3}\mathrm{H}(\frac{1}{2}^{+};\frac{1}{2})\ (\beta^{-})\ ^{3}\mathrm{He}(\frac{1}{2}^{+};\frac{1}{2})$						
0.0186	1.41404 (0)	1.41444 (14)	2.2752 (1)	2.2446 (13)	2.317 (4)	
$^{6}\mathrm{He}(0^{+};1)\ (\beta^{-})\ ^{6}\mathrm{Li}(1^{+};0)$						
3.508			2.1761 (13)	2.161 (7)	2.174 (3)	2.182 (3)
$^{7}\mathrm{Be}(\frac{3}{2}^{-};\frac{1}{2})\ (\epsilon)\ ^{7}\mathrm{Li}(\frac{3}{2}^{-};\frac{1}{2})$						
0.8618	1.99980 (2)	2.0003 (5)	2.3348 (6)	2.296 (4)	2.280 (3)	2.290 (4)
$^{7}\mathrm{Be}(\frac{3}{2}^{-};\frac{1}{2})\ (\epsilon)\ ^{7}\mathrm{Li}(\frac{1}{2}^{-};\frac{1}{2})$						
0.3842			2.1499 (5)	2.087 (10)	2.119 (6)	2.128 (8)
Branching ratio						
			0.1038 (5)	0.1005 (10)	0.1039	
$^{10}\mathrm{C}(0^{+};1)\ (\beta^{+})\ ^{10}\mathrm{B}(1^{+};0)$						
1.9076			2.063 (3)	2.026 (21)	1.854 (2)	1.862 (2)
$^{10}\mathrm{C}(0^{+};1)\ (\beta^{+})\ ^{10}\mathrm{B}(1^{+}_{2};0)$						
0.4717			0.451 (14)	0.354 (45)	(< 0.9)	
Branching ratio						
			0.0029 (2)	0.0019 (5)	(< 0.0008)	

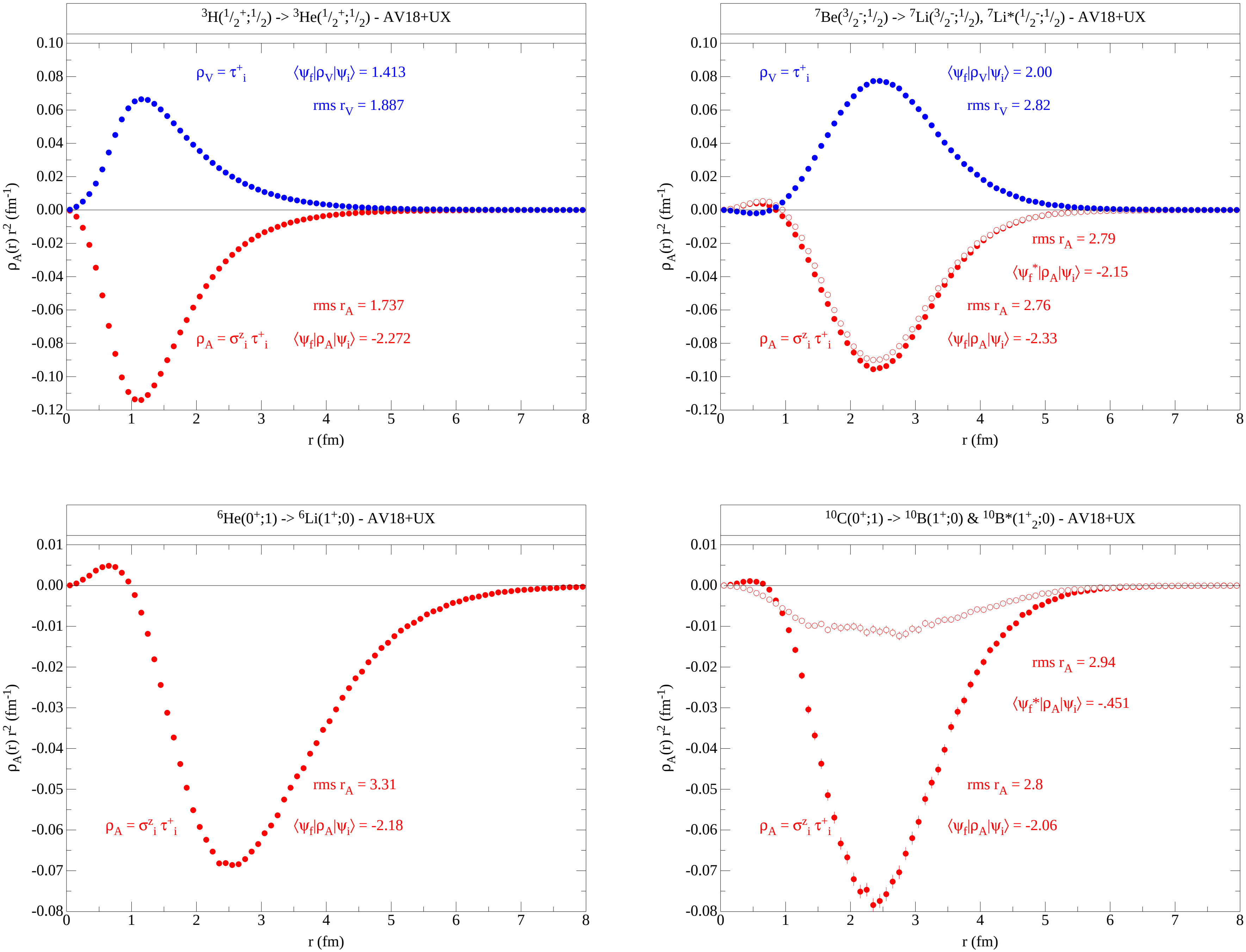

3H(1/2+;1/2) -> 3He(1/2+;1/2) - AV18+UX
ρV = τ+i
⟨ψf|ρV|ψi⟩ = 1.413
rms rV = 1.887
rms rA = 1.737
ρA = σzi τ+i
⟨ψf|ρA|ψi⟩ = -2.272
7Be(3/2-;1/2) -> 7Li(3/2-;1/2), 7Li*(1/2-;1/2) - AV18+UX
ρV = τ+i
⟨ψf|ρV|ψi⟩ = 2.00
rms rV = 2.82
rms rA = 2.79
⟨ψf*|ρA|ψi⟩ = -2.15
rms rA = 2.76
ρA = σzi τ+i
⟨ψf|ρA|ψi⟩ = -2.33
6He(0+;1) -> 6Li(1+;0) - AV18+UX
rms rA = 3.31
ρA = σzi τ+i
⟨ψf|ρA|ψi⟩ = -2.18
10C(0+;1) -> 10B(1+;0) & 10B*(1+2;0) - AV18+UX
rms rA = 2.94
⟨ψf*|ρA|ψi⟩ = -.451
rms rA = 2.8
ρA = σzi τ+i
⟨ψf|ρA|ψi⟩ = -2.06
ρA(r) r2 (fm-1)
r (fm)

Benchmark for $0\nu\beta\beta$ decay